Vol.5, No.2 pp. 546-558
ISSN 1805-3602

Calibration of separate window model factors to calculate land surface temperature using MODIS images

Sadegh Modiri[1*], Mahdi Modiri[2]
[1]Geomatics Engineering- University of Stuttgart, Stuttgart, Germany; [2]Institute of Surveying and Mapping and Head of National Geographical Organization, Tehran, Iran
[*]E-mail: sadeghamiri122@gmail.com

Received for publication: 20 February 2016.
Accepted for publication: 25 May 2016.

Abstract

Land surface temperature (LST) is one of the most important parameters influencing physical processes of energy on the land surface and in high seas, both in local and global scales. Satellite infrared temperature data (TIR) is linked directly to LST using radiation transmission models. However, direct estimation of LST from radiation in TIR spectrum will be of low accuracy. Since the radiation measured by satellites depends not only on land surface parameters (temperature and irradiance power) but also on atmospheric influences. LST calculation suggests different methods for decreasing atmospheric influences, which can be classified in three major classes: single band methods, multiple band methods, and multiple angle methods. The present article investigates multi-temporal data of MODIS images in 12 different dates with quite uniform temporal distribution during 2014 using five useful multiple band methods of calculating LST including, Price Model (1994), Becker and Li Model (1990), Platt and Prata Model (1991), Ulivieri et al. model (1994), Coll et al. model (1994). Then, coefficients of investigated models were calibrated using the least repetitive squares model. During the calibration, main coefficients of the models were used as the initial value and optimal coefficients were calculated using a series of data. Afterward, the accuracy of the modified models was evaluated using LST from MODIS and the Iranian weather stations data. Results illustrate the modified Price Model by an average of RMSE 0.41 Centigrade degree as the most accurate model. Moreover, the variance of RMSE is 0.08 for mentioned dates which confirm generalizability of the outcomes. The maximum and minimum of RMSE equals 0.26 and 0.50 respectively (February 19th and June 27th respectively) for modified Price model. Finally, the linear relation was investigated, between LST calculated using modified Price Model and data measured by Iranian weather stations.

The linear regression factor of these two series of data was 0.9978 which indicates a significant linear relation between calculated LST data and reference temperatures of the Iranian weather stations.

Keywords: Land Surface Temperature, least repetitive squares, optimization, MODIS images

Introduction

Land surface temperature (LST) is one of the most important parameters influencing physical processes of energy on land surface and in high seas, both in local and global scales (Anderson et al., 2008; Brunsell and Gillies, 2003; Karnieli et al., 2010; Kustas and Anderson, 2009; Zhang et al., 2008). Knowledge of LST provides information about the thermal balance level of surfaces, which is of special importance in many different research grounds such as evapotranspiration, climate change, hydrological cycles, plant monitor, urban climate and

environmental studies (Arnfield, 2003; Bastiaanssen et al., 1998; Hansen et al., 2010; Kalma et al., 2008; Kogan, 2001; Su, 2002; Voogt and Oke, 2003; Weng, 2009; Weng et al., 2004). Because of high heterogeneity in land surface, features such as vegetation, topography and soil type (Liu et al., 2006; Neteler, 2010), LST has dramatic temporal and local changes (Prata et al., 1995; Vauclin et al., 1982). As a result, accurate determination of surface temperature and its temporal changes requires measuring LST with appropriate local and temporal sampling (Li et al., 2013). Recently, Satellite data has provided temporal and local measurement of LST for glob (Li et al., 2013; Pahlevani and Mobasheri, 2009). The satellite thermal infrared data (TIR) is directly related to LST using radiation transmission models and since 1970, it attracts much attention (McMillin, 1975). However, estimation of LST directly from radiation in TIR spectrum will be of low accuracy. Since the radiation measured by satellites depends not only on land surface parameters (temperature and irradiance power) but also on atmospheric influences (Li and Becker, 1993; Ottlé and Stoll, 1993; Prata et al., 1995). Therefore, apart from radiometric calibration of sensors and cloud mask of satellite image, irradiance power and atmospheric correction are also required for calculating LST (Li and Becker, 1993; Vidal, 1991). Many studies have been performed in this realm and many methods have been suggested for estimation of surface irradiance power and atmospheric effect compensation in order to calculate LST using satellite TIR data (Becker and Li, 1990b; Gillespie et al., 1998; Hook et al., 1992; Jiménez-Muñoz and Sobrino, 2003; Kealy and Hook, 1993; Kerr et al., 1992; Pozo Vazquez et al., 1997; Price, 1983, 1984; Qin et al., 2001; Susskind et al., 1984; Tonooka, 2001; Wan and Dozier, 1996; Wan and Li, 1997). In this article, after describing the foundations of LST calculation from thermal images, different methods of calculating LST including single band method, separate window method and multiple angle method were investigated. Five useful methods of separate window were selected and their operations in a series of multi temporal data of MODIS images were investigated. Finally, the coefficients of the models were calibrated using the repetitive least square model. Also, the accuracy of modified models were investigated based on the LST data from MODIS and data of Iranian weather stations.

Study Area and Data

Study Area

The study area of this research is Iran which located in Middle East (figure 1).

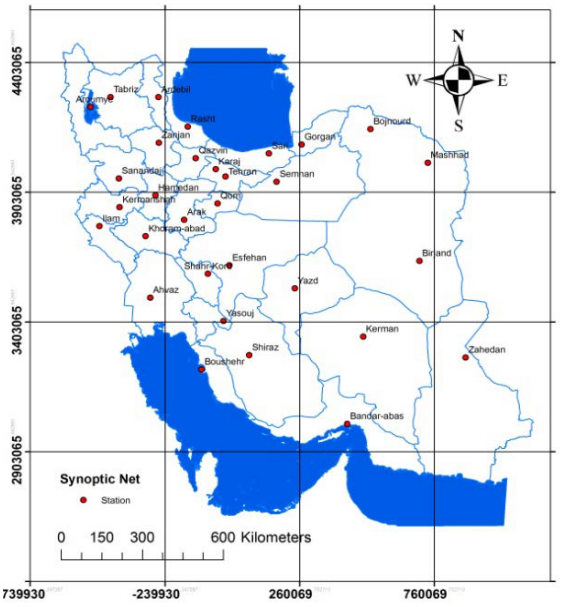

Figure 1: the study area

This country with lots of topographic and climatic diversity is located between 25 to 40 degree longitude and 44 to 64 degree latitude

Data

MODIS Images

MODIS satellite has 36 spectral bands. Due to global coverage, high temporal and spectral separation power, appropriate dynamic interval and accurate calibration in several thermal bands which are specifically designed for sea surface temperature (SST), LST and atmospheric parameters, this sensor is of significant importance. In the present research, 12 series of B1 level images of AQUA sensor for MODIS satellite (figure 2) with quite uniform temporal distribution in 2014 were studied (table 1). These images are freely accessible on http://wist.echo.nasa.gov/.

Table 1: data which are used in 2014

Image #	Julian Day	Date
01	002	Jan 02, 2014
02	050	Feb 19, 2014
03	082	Mar 23, 2014
04	114	Apr 24, 2014
05	146	May 26, 2014
06	178	Jun 27, 2014
07	210	Jul 29, 2014
08	242	Aug 30, 2014
09	258	Sep 15, 2014
10	275	Oct 01, 2014
11	306	Nov 02, 2014
12	338	Dec 04, 2014

Cloud Mask Output and MODIS Research Team for LST

LST production of MODIS research team was used to evaluate the accuracy of calculated LST (figure 2). In order to compare calculated LST and LST product of MODIS research team, images were masked using Cloud mask output of MODIS research team (figure 2). These productions are freely accessible on http://wist.echo.nasa.gov/.

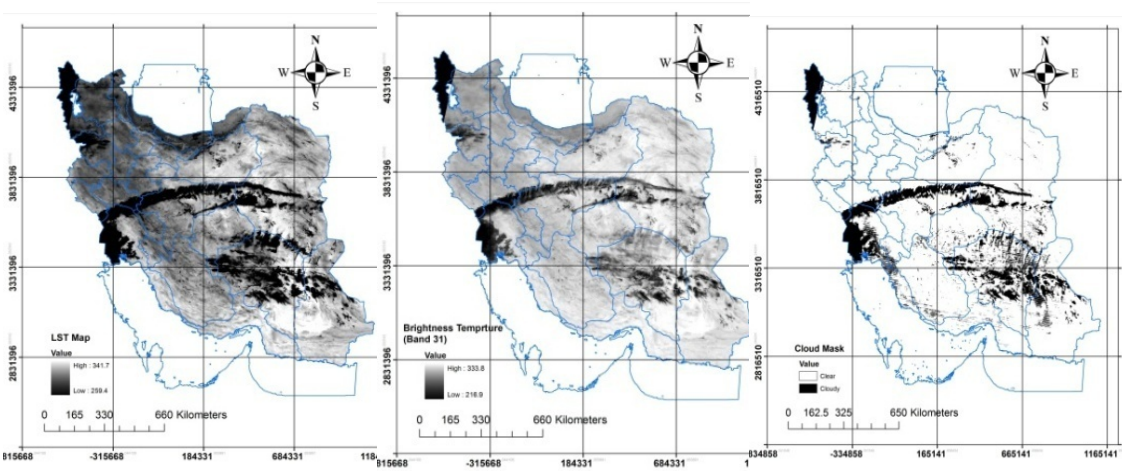

Figure 2: (a) B1 level image of AQUA sensor, (b) LST output, (c) cloud mask output of MODIS research team on 16th may 2014

Meteorological data

Due to lack of access to LST data in this area, local weather stations were used for validation of research outcome using the measured temperature near to Earth surface. These data were collected for each weather station on the day of retrieving satellite images from meteorological organization website http://www. irimo.ir/eng/wd/720-Products-Services.html at 6 am and 9 am UTC. The satellite pass Iran at 10:30 according to Tehran time. Therefore, meteorological data at the time that satellite is passed was calculated based on the linear interpolation on these two data series (table 2).

Table 2: Meteorological data interpolated for the time of satellite pass

Station	Julian Day, Year 2014											
	002	050	082	114	146	178	210	242	258	275	306	338
Arak	7.7	10	26.7	28.3	31	27.7	31	25.7	19.3	7	8	-2
Ardebil	-3	9.7	12.7	17	20.7	19.3	24.7	24	15	5	1.7	-1.7
Uromye	3.3	14	19	24.7	30	24.7	28	23.3	18	11.7	8	-0.7
Esfahan	11	15.3	29	29	31	33	34	28.3	19.3	9.7	9.3	0.7
Ahvaz	19.7	30.3	36.7	35.7	39	38	40.3	37.3	31	24	18	14.7
Ilam	14.7	11	28	30	34	32.7	33	29	20	15	8.7	5.3
Bojnourd	0.3	9.7	22.3	26.7	29.7	26.7	31.3	30	14	-0.7	6.7	0.7
Bandarabas	27.3	29	33.3	34.3	34	35.7	34.7	38.3	30.3	26.7	22	20
Boushehr	20.3	27	34	34	36.7	34	35.7	33.3	27.7	22	18	16.3
Birjand	12	17.3	32	31.7	30.7	36.3	36	31	24	6.3	9	8
Tabriz	2.7	11.7	18.3	24.3	30	24.7	29.7	23	16.3	11.3	7.3	-1.7
Tehran	8	12.7	29	31.7	34	29	33.3	29.3	20.3	7	9.7	1.3
Khoramabad	13.3	11.3	29.7	30.3	35.7	34.7	34	30	20.7	14.7	8.3	4.7
Rasht	9	17.3	18.3	27.3	30	26.7	30.7	27.3	19.3	12	9	6.7
Zahedan	13.7	23.3	31.7	31.7	32	37.7	36	33.3	29	13	13.3	11.3
Zanjan	0.7	11.3	24	25.7	30.7	23.3	25.7	22	16	6.3	5.3	-1
Sari	7.7	18.7	21.3	26.3	33	25	31	28.3	18	10.3	18.7	8.7
Semnan	7.3	14	30.3	33.3	33.7	34	38	34.3	22.3	6	11.3	0.7
Sanandaj	10	11	25.3	27.7	33	29	32.7	26.3	20	10.3	4.3	1.3
Shahre Kord	4.3	12.3	24	27.7	26.7	32	28	24.3	18	8.7	2.7	-1
Shiraz	14.3	17.7	29.3	30	31	35.7	34.3	31	25	14.7	9	4
Qazvin	3.7	12.7	25.7	29	30.3	28	32.7	28	21	10.3	10	-0.3
Qoum	10.3	14	32.3	32	35.3	32.7	38	33.7	24.7	12.3	13.3	1.3
Karaj	4	11.7	24.7	29	30.3	24.7	30.7	27	18.7	6	8.7	0.7
Kerman	12.7	18.7	30.3	30	28.7	38	34.7	30.7	25	6.3	10.3	8.3
Kermanshah	10	12.3	25.7	27.7	34	31.7	32.7	26.7	19.7	11.7	4	3.3
Gorgan	7	17.3	24.3	30	33	25.7	31	30.3	19.3	11	18.3	6.7
Mashhad	0	16.3	24.3	30.3	32.7	29.3	35.7	32.3	20	1.3	10.3	5
Hamedan	7.3	10.7	24	26.3	29.7	26.3	28.3	24	17.3	7	3.4	-0.7
Yasouj	9.7	14	26	28.3	28.3	33	30	27	21	10.3	-1	-1.7
Yazd	11	20.7	23.3	31.7	32.7	33.7	38	32.3	26.7	9.7	12	2

LST Calculation

Theoretical Background

All objects with temperature more than 0 Kelvin emits thermal energy and radiation level of a black object with thermal balance in λ wavelength and T temperature can be calculated using Plank relation:

$$B_\lambda(T) = \frac{C_1}{\lambda^5\left[\exp\left(\frac{C_2}{\lambda T}\right)-1\right]} \quad (1)$$

Where, Bλ(T) is spectral radiance(W m−2 μm−1 sr−1) of black object in T (K)temperature and λ (μm) wave length; C1 and C2 are physical constants (C1=1.191×108Wμm4sr−1 m−2, C2=1.439×104 μm•K).

Since most of the natural objects are not black, their ε irradiance power which is defined as the ratio of one object radiance to its black isothermal object radiance must be considered. Spectral radiance of a non-black object can be calculated by multiplication of irradiance power in its black isothermal object (Equation 1). Obviously, if the atmosphere had no influence on satellite views, surface LST could be calculated for certain irradiance power and radiation radiance. But in reality, in order to calculate surface LST accurately from satellite images, apart from irradiance power of the surface, we need to correct atmospheric influences. Different methods were suggested for these corrections since the 1970s most of which can be classified in three major groups: single band methods, separate window methods and multiple angle methods.

Single band method

In this method, only a single thermal band is used for calculating LST (Weng 2009). Therefore, methods can be implemented using sensors such as Landsat 7/ETM + and Meteosat-MVIRI which only possess a single thermal band. In these methods, reverse atmospheric transport models are used for correction of atmospheric influences and thus humidity, temperature and atmospheric pressure profiles are needed for precise outcomes.

Separate Window Method

In these methods, a linear combination of two adjacent thermal bands' radiance is used for correction of atmospheric influences (Zhang et al., 2006). It is assumed that changes in the irradiance power of surfaces in two adjacent thermal bands are insignificant, and the change in temperature is a result of atmospheric influences. In order to implement these methods, the used sensor must have at least two thermal bands. MODIS, AVHRR, ASTER and LandSAT 8 can be referred to as instances of these sensors.

Multiple Angle Method

In these methods, it assumes that there are not many local changes and combination of multiple angle views of a phenomenon in a spectral band is used for correction of atmospheric influences (Prata and Platt, 1991). These views are accessible from sensors such as Meteosat and TIROS-N. When irradiance power of surface in different wavelengths changes continuously, this method is quite more accurate compared to separate window method.

Methodology

The present article takes advantage of five useful models of a separate window as referred to in different scientific papers (table3). In the beginning phase, selected models were implemented using coefficients proposed by the authors and the accuracy of their results was evaluated using LST output of MODIS research team. Then, the coefficients of these models were calibrated using the least repetitive square model. In the calibration process, models main coefficients were used as the initial value and improved coefficients were calculated using thermal images and LST output of

MODIS research team on January 2d 2014. The accuracy of other 11 series of improved models was evaluated with LST output of MODIS research team and data records in weather stations.

Table 3: selected separate window models

Authors	LST Model*
Price (1984)	$LST = A_0 + A_1 T_{11} + A_2 (T_{11} - T_{12}) + A_3 T_{11} \varepsilon_{11} + A_4 (T_{11} - T_{12})(1 - \varepsilon_{11}) + A_5 T_{12} \Delta\varepsilon$
Becker and Li (1990)	$LST = A_0 + \left(A_1 + A_2 \frac{1-\varepsilon}{\varepsilon} + A_3 \frac{\Delta\varepsilon}{\varepsilon^2} \right)(T_{11} + T_{12}) + \left(A_4 + A_5 \frac{1-\varepsilon}{\varepsilon} + A_6 \frac{\Delta\varepsilon}{\varepsilon^2} \right)(T_{11} - T_{12})$
Prata and Platt (1991)	$LST = A_0 + A_1 \frac{T_{11} - T_0}{\varepsilon_{11}} + A_2 \frac{T_{12} - T_0}{\varepsilon_{12}} + A_3 \frac{1 - \varepsilon_{11}}{\varepsilon_{11}} + T_0$
Ulivieri et al. (1994)	$LST = A_0 + A_1 T_{11} + A_2 (T_{11} - T_{12}) + A_3 (1 - \varepsilon) + A_4 \Delta\varepsilon$
Coll et al. (1994)	$LST = A_0 + A_1 T_{11} + (A_2 + A_3 (T_{11} - T_{12}))(T_{11} - T_{12}) + A_4 (1 - \varepsilon) + A_5 \Delta\varepsilon$

• In these equations T11 and T12 are radiating temperature in 11 and 12 micron wave length, ε11 and ε12 are irradiance power in 11 and 12 micron wavelength, ε and Δε are average and changing range of ε11 and ε12 ،T0 = 273.15 ˚K respectively and finally Ai are also models coefficients.

Radiating temperature in 11 and 12 micron wave length were calculated using 31 and 32 sensor bands of MODIS. NDVI method was used to estimate irradiance power in these two wave lengths (Sobrino and Raissouni, 2000; Lyon, 1965; Valor and Caselles 1996):

$$\varepsilon_i = \varepsilon_{vi} P_v + \varepsilon_{si} (1 - P_v) + C_i \quad (2)$$

Where, εvi and εsi are spectral irradiance power for vegetation and bare soil, Pv is vegetation coefficient and Ci is a reparative term used as a consideration for empty space between vegetation canopy which depends on structure and geometry of the canopy. In homogeneous places, this term can be considered zero (Sobrino et al., 2001). Pv value can be calculated using NDVI index (Valor and Caselles, 1996):

$$P_v = \left(\frac{NDVI - NDVI_s}{NDVI_v - NDVI_s} \right)^2 \quad (3)$$

Where, NDVIv and NDVIs are NDVI value for luxuriant vegetation (Pv=1) and bare soil (Pv = 0) respectively, which can be extracted from NDVI histogram.

Results and Discussion

First, selected methods were implemented using main coefficients published by authors (table 4).

Table 4: main coefficients published for selected models

LST Model	Parameters	Original Coefficients
Price (1984)	[A0~A5]	[0,1,3.33,5.5,4.5,0.75]
Becker and Li (1990)	[A0~A6]	[1.274,1,0.15616,-0.482,6.26,38.33]
Prata and Platt (1991)	[A0~A3]	[0,3.45,-2.45,40]
Ulivieri et al. (1994)	[A0~A4]	[0,1,1.8,48,-0.75]
Coll et al. (1994)	[A0~A5]	[0,1,0.85,40,-75]

The accuracy of calculated LST was evaluated pixel by pixel in comparison with LST output of MODIS research team. Before comparing these two series of data, calculated LSTs were masked using cloud mask output of MODIS. Resulting RMSE error of models is presented in table 5.

Table 5: the accuracy of selected models based on comparison with LST output of MODIS research team

Julian Day	LST Model				
	Price (1984)	Becker & Li (1990)	Prata & Platt (1991)	Ulivieri et al. (1994)	Coll et al. (1994)
002	1.88	3.45	58.9	21.6	17.7
050	2.04	2.96	64.4	21.3	17.5
082	2.14	3.41	68.5	21.2	17.4
114	2.45	3.55	82.6	20.7	16.7
146	2.45	4.09	90.1	20.8	16.7
178	2.42	4.57	93.2	20.9	17.0
210	2.51	4.62	91.4	20.6	16.6
242	2.50	4.32	89.9	20.8	17.0
258	2.51	4.33	87.5	20.8	16.9
275	2.43	4.00	84.4	20.8	16.9
306	2.30	3.32	74.1	20.9	16.8
338	1.99	3.00	63.0	21.4	17.6

Based on table 5, Price model (1984) and Prata and Platt (1991), with average RMSE of 2.30 and 79.00 centigrade respectively, formed the best and the worst results. Figure 3 compares average and RMSE standard deviation of models.

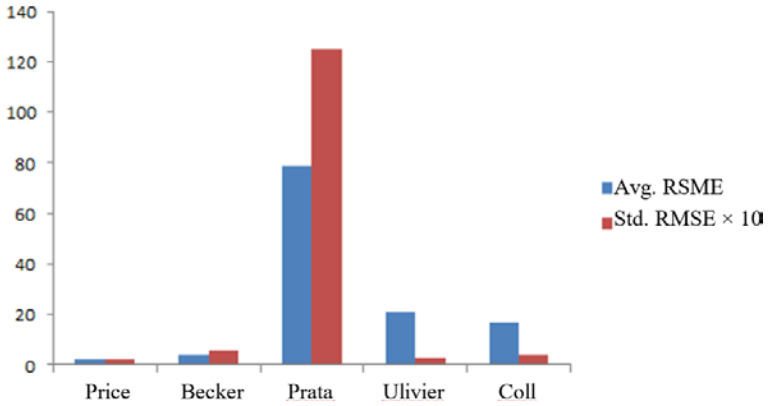

Figure 3: Average and RMSE standard deviation of different models

Figure 3 illustrate regardless of accuracy, all models except for Prata and Platt (1991) have low RMSE standard deviation.

Table 6: improved coefficients of models according to least repetitive square model

LST Model	Parameters	Optimized Coefficients
Price (1984)	[A0~A5]	[-2.892,1.088,-0.146,4.19,0.449]
Becker and Li (1990)	[A0~A6]	[-2.79,0.96,0.0530.0996,21.83,-15.89]
Prata and Platt (1991)	[A0~A3]	[-20.447,1.335,-0.8605,21.1182]
Ulivieri et al. (1994)	[A0~A4]	[-40.165,1.011,1.8406,76.37,59.096]
Coll et al. (1994)	[A0~A5]	[-38.42,1.012,1.799,72.444,61.46]

Therefore, seemingly their accuracy can be significantly improved by adding a fixed term. As table 4 shows, this fixed term equals zero in all models except for Becker and Li (1990) model. Thus, a fixed term was added to the other four models before calibrating models' coefficients. Then, models' coefficients were calibrated considering models' main coefficients as the initial value and using the repetitive least square model and (table 6).

The accuracy of modified models was evaluated in comparison with LST output of MODIS research team. RMSE of improved models is presented in table 7.

Table 7: the accuracy of improved models compared to LST output of MODIS research team

Julian Day	LST Model				
	Price (1984)	Becker & Li (1990)	Prata & Platt (1991)	Ulivieri et al. (1994)	Coll et al. (1994)
002	0.32	0.33	0.39	0.27	0.26
050	0.26	0.26	0.40	0.27	0.29
082	0.34	0.34	0.57	0.41	0.36
114	0.46	0.47	0.86	0.70	0.57
146	0.43	0.43	1.15	0.71	0.59
178	0.50	0.57	1.22	0.74	0.66
210	0.49	0.55	1.20	0.74	0.63
242	0.48	0.49	1.17	0.73	0.61
258	0.44	0.44	1.09	0.69	0.58
275	0.47	0.48	0.98	0.68	0.56
306	0.49	0.50	0.73	0.66	0.51
338	0.28	0.28	0.39	0.28	0.29

According to table 8, Price improved model (figure 4) and Prata and Platt improved model showed the best and worst result, with average RMSE of 0.41 and 0.81 respectively. But unlike the main models, nearly all improved models reached accuracy less than one.

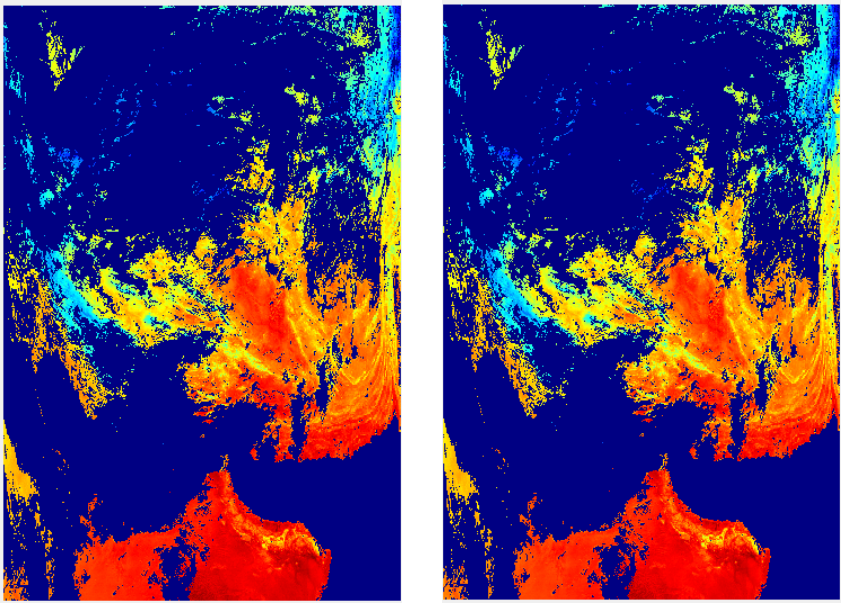

Figure 4: (a) LST calculated using improved Price model, (b) LST output of MODIS research team on January 2d 2014

Average and standard deviation of RMSE for modified models are presented in figure 5.

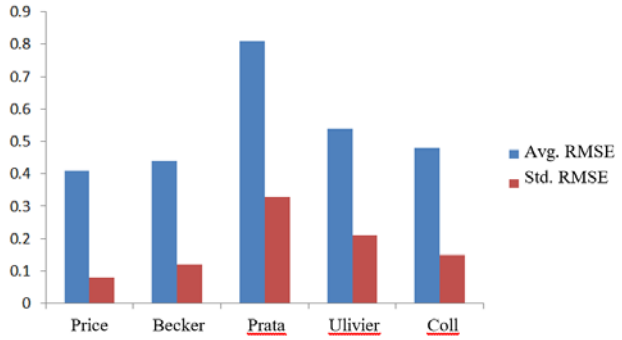

Figure 5: Average and RMSE standard deviation of improved models

Table 8: calculated LST using modified Price model in the position of weather stations

Station	Julian Day, Year 2014											
	002	050	082	114	146	178	210	242	258	275	306	338
Arak			37.2	40.3	46	39.1	44.4	36.9	27.9	22.4	14	
Ardebil						29.7	35.2	33.4		18.9		
Uromye		9.2	21.6	27.9	31.2	25	27.6	23.6	17.5	7.8		
Esfahan	11.4	20.6	37.8	38.3	43	41.7	45.7	39	28.4	21.1		
Ahvaz		34.1	43.5	44	42.5	49.9	49.6		41.6	31.3		19.9
Ilam	9.7		32	42.6	39	40.2	42.4	38.3	27.6	18	20.6	
Bojnourd	5.1		33.8	38.8	43.4	50.2	48.1	47.3	18			
Bandarabas	33.2	36	40	43.7	45.1	45.5	49.5	52.9	43.7	32	30.1	
Boushehr		30.6	40.1	36.7	38.2	44.2		46.6	30.1	26.9		
Birjand	16.3		41.5	49.4	51	51.1	52.9	41.3	35.7	14	13.4	22.7
Tabriz			26.8	31.4		34.4	38.1	33.8	25.5	22.5		
Tehran		18.3	38.1	43.1	47	37.3	47.7	44	32.4		18.3	
Khoramabad			38.7	41.4	47.4	43.6	47.1	40.1	27.3	21		
Rasht	12.2							31.4		20.2		
Zahedan	20.7	30.6	45.4	50.9	50.5	48.4	53.4		44.8		24.4	21.8
Zanjan		11	35	36.1	41.5	34.7	37.5	31.5	23.5	20.4		
Sari	13.3				36.9		36.1				23.5	
Semnan			35.7	42.5	44.7	47.1	49	43.3	35.8			
Sanandaj	13.8		34.1	42.4	43.6	42.1	42.9	29	31.1	25		
Shahre Kord	4.7	15.8	42.9	41	42.8	49		39.1	27.7	25.5	10.8	0.7
Shiraz	16.8	24.6	44.4		45.6	50	47.6	47.3	38.1	27.6		
Qazvin			34.1	35.3	41.7		36.7	41.9		23.9		
Qoum			38.5	42.3	46.6		48.2	42.7	31.9	21.5		
Karaj	13.6		41.6	42	48.6	35.3	45	44.1	28.3	23.1	15.3	-5.5
Kerman	19.9		43.5	47.3	49.4	55.9	53.7	40	42.2		18.9	20.6
Kermanshah			33.6	37.6	45.8	43.8	44.4	39	31.8	21.3		
Gorgan	10.7			37.5	35.2			36.9			23.8	
Mashhad		19.3	30.3	40.6	43.3	42.9	50.4	44.4	30			
Hamedan	11.9		37.4	40.9	44.2	39.6	33.4	36.5	32.9	24.2	1.5	
Yasouj		20.2	38.8	39.2	41.8	43.4	44.5	41	30.6	22.1		1.1
Yazd	16.7	24.7	43.6	47.1	49.1	47	55.7	49.5	43.4	27.9	22.6	

Modified Price model possessed, apart from the least RMSE average, the least RMSR standard deviation which shows generalizability of model results in the temporal range. For an applied evaluation of improved Price model, calculated LST values of local weather stations' positions were extracted (table 8).

Finally, linear relation of calculated LST and thermal values recorded in weather stations was investigated using modified Price model (figure 6).

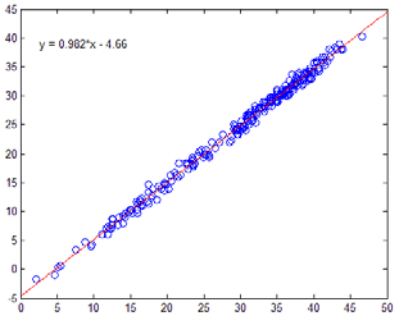

Figure 6: linear relation of calculated LST and values measured in weather stations using modified Price model

The coefficient of determination resulted from linear regression of these two data series equaled 0.9978 which shows high linear correlation. Thus, it seems that LST values resulted from this models can be used for estimation of temperature near earth surface.

Conclusion

Earth surface temperature is one of the most important environmental parameters influencing physical processes of energy on earth and in high seas, both in local and global scale. By development of satellite remote sensing, satellite data has provided the possibility of local and temporal measurement of LST all over the earth. Satellite thermal infrared (TIR) data are directly related to LST using radiation transfer models. Yet, direct estimation of LST from radiation in TIR spectrum will be of low accuracy. Since radiation measured by satellite, sensors depends not only on earth surface parameters (temperature and irradiance power) but also on atmospheric influences. As a result, in addition to radiometric calibration of sensors and cloud mask of satellite images, irradiance power of surfaces and atmospheric corrections are needed for calculation of LST from satellite TIR images. Many studies have been performed on the issue and many methods have been proposed for estimation of surface irradiance power and correction of atmospheric influences to calculate LST using satellite TIR data, most of which can be classified in 3 major forms: single band method, separate window method and multiple angle method.

In the present article, after describing different methods of calculating LST, five useful methods of the separate window to which different scientific papers have referred were selected and their operation on a series of multi-temporal data of MODIS images was investigated. Results indicate that Price model (1984) and Prata and Platt (1991) model with average RMSE of 2.30 and 79.00 centigrade respectively showed the best and worst results. Apart from accuracy, all models except for Prata and Platt (1991) had low RMSE standard deviation. As a result, it seemed that adding a fixed term can improve their accuracy to a significant level. Therefore, a fixed term was added to the other four models before calibration of models coefficients. Then, models coefficients were calibrated using least repetitive square model and the main models' coefficients as the initial value. Then, coefficients of these models were calibrated using least repetitive square model and the accuracy of improved models was evaluated in the other 11 data series based on LST output of MODIS research team. According to table 8, again improved Price model (figure 4) and improved

Platt and Prata model with average RMSE of 0.41 and 0.81 showed the best and the worst results. But unlike the main models, nearly all improved ones reached accuracy less than one. Improved Price model had, in addition to the least average RMSE, the least RMSR standard deviation which shows generalizability of results in the temporal period. Finally, linear relation of calculated LST was investigated using improved Price model and thermal values measured in weather stations. The coefficient of determination resulted from linear regression of the two data series equaled 0.9978 which shows high correlation. Thus, it seems that LST values resulted from this model can be used for estimation of weather temperature near earth surface.

References

Anderson, M. C., Norman, J. M., Kustas, W. P., Houborg, R., Starks, P. J., and Agam, N. (2008). A thermal-based remote sensing technique for routine mapping of land-surface carbon, water and energy fluxes from field to regional scales. Remote Sensing of Environment, 112, pp. 4227–4241.

Arnfield, A. J.(2003). Two decades of urban climate research: a review of turbulence, exchanges of energy and water, and the urban heat island. International Journal of Climatology, 23, pp. 1–26.

Bastiaanssen, W. G. M., Menenti, M., Feddes, R. A., and Holtslag, A. A. M.(1998). A remote sensing surface energy balance algorithm for land (SEBAL). Journal of Hydrology, 212, pp. 198–212.

Becker, F., and Li, Z.-L.(1990). Towards a local split window method over land surfaces. International Journal of Remote Sensing, 11, pp. 369–393.

Brunsell, N. A., and Gillies, R. R.(2003). Length scale analysis of surface energy fluxes derived from remote sensing. Journal of Hydrometeorology, 4, pp. 1212–1219.

Coll, C., Caselles, V., Sobrino, A., and Valor, E.(1994). On the atmospheric dependence of the split-window equation for land surface temperature. Int. J. Remote Sens., 15, pp. 105-122.

Gillespie, A. R., Rokugawa, S., Matsunaga, T., Cothern, J. S., Hook, S., and Kahle, A. B. (1998). A temperature and emissivity separation algorithm for Advanced Spaceborne Thermal Emission and Reflection Radiometer (ASTER) images. IEEE Transactions on Geoscience and Remote Sensing, 36, pp. 1113–1126.

Hansen, J., Ruedy, R., Sato, M., and Lo, K.(2010). Global surface temperature change. Reviews of Geophysics, 48, RG4004.

Hook, S. J., Gabell, A. R., Green, A. A., and Kealy, P. S.(1992). A comparison of techniques for extracting emissivity information from thermal infrared data for geologic studies. Remote Sensing Environment, 42, pp. 123–135.

Jiménez-Muñoz, J. C., and Sobrino, J. A.(2003). A generalized single-channel method for retrieving land surface temperature from remote sensing data. Journal of Geophysical Research, 108, pp. 4688–4695.

Kalma, J. D.,McVicar, T. R., and McCabe,M. F.(2008). Estimating land surface evaporation: A review of methods using remotely sensed surface temperature data. Surveys in Geophysics, 29, pp. 421–469.

Karnieli, A., Agam, N., Pinker, R. T., Anderson, M., Imhoff, M. L., and Gutman, G. G. (2010). Use of NDVI and land surface temperature for drought assessment: Merits and limitations. Journal of Climate, 23, pp. 618–633.

Kealy, P. S., and Hook, S. J. (1993). Separating temperature and emissivity in thermal infrared multispectral scanner data: Implications for recovering land surface temperatures. IEEE Transactions on Geoscience and Remote Sensing, 31, pp. 1155–1164.

Kerr, Y. H., Lagouarde, J. P., and Imbernon, J. (1992). Accurate land surface temperature retrieval from AVHRR data with use of an improved split window algorithm. Remote Sensing of Environment, 41, pp. 197–209.

Kogan, F. N.(2001).Operational space technology for global vegetation assessment. Bulletin of the American Meteorological Society, 82, pp. 1949–1964.

Kustas, W., and Anderson, M.(2009).Advances in thermal infrared remote sensing for land surface modeling. Agricultural and Forest Meteorology, 149, pp. 2071–2081.

Li, Z.-L., and Becker, F.(1993).Feasibility of land surface temperature and emissivity determination from AVHRR data. Remote Sensing of Environment, 43, pp. 67–85.

Li, Zh., Tang, B., Ren, H., Yan, G., Wan, Zh., Trigo, I., and Sobrino, J.(2013). Satellite-derived land surface temperature: Current status and perspectives. Remote Sensing of Environment, 131, pp. 14–37.

Liu, Y., Hiyama, T., and Yamaguchi, Y. (2006). Scaling of land surface temperature using satellite data: A case examination on ASTER and MODIS products over a heterogeneous terrain area. Remote Sensing of Environment, 105, pp. 115–128.

Lyon, R.J.P.(1965). Analysis of rocks by spectral infrared emission (8 to 25 microns), Economic Geology, 60, pp. 715−736.

McMillin, L. M. (1975). Estimation of sea surface temperature from two infrared window measurements with different absorptions. Journal of Geophysical Research, 80, pp. 5113–5117.

Neteler, M. (2010). Estimating daily land surface temperatures in mountainous environments by reconstructed MODIS LST Data. Remote Sensing, 2, pp. 333–351.

Ottlé, C., and Stoll, M. (1993). Effect of atmospheric absorption and surface emissivity on the determination of land surface temperature from infrared satellite data. International Journal of Remote Sensing, 14, pp. 2025–2037.

Pahlevani, M., Mobasheri, M.R.(2009). An Improvement on Land Surface Temperature Determination by Producing Surface Emissivity Maps. Desert, pp. 171-184.

Pozo Vazquez, D., Olmo Reyes, F. J., and Alados Arboledas, L.(1997). A comparative study of algorithms for estimating land surface temperature from AVHRR data. Remote Sensing of Environment, 62, pp. 215–222.

Prata, A. J., and Platt, M. (1991). Land surface temperature measurements from the AVHRR. In: Proceedings of the 5th AVHRR data Users' Meeting. Tromso (NORWAY). 24-28 June EUMETSAT, Darmstadt, pp. 433-438.

Prata, A. J., Caselles, V., Coll, C., Sobrino, J. A., and Ottlé, C.(1995). Thermal remote sensing of land surface temperature from satellites: Current status and future prospects. Remote Sensing Reviews, 12, pp. 175–224.

Price, J. C.(1983). Estimating surface temperatures from satellite thermal infrared data: A simple formulation for the atmospheric effect. Remote Sensing of Environment, 13, pp. 353–361.

Price, J. C.(1984). Land surface temperature measurements from the split window channels of the NOAA 7 AVHRR. Journal of Geophysical Research, 89, pp. 7231–7237.

Qin, Z., Karnieli, A., and Berliner, P. (2001). A mono-window algorithm for retrieving land surface temperature from Landsat TM data and its application to the Israel-Egypt border region. International Journal of Remote Sensing, 22, pp. 3719–3746.

Sobrino, J.A. and N. Raissouni.(2000). Toward remote sensing methods for land cover dynamic monitoring, Application to Morocco, International Journal of Remote Sensing, 21, pp. 353−366.

Sobrino, J.A., N. Raissouni and Z.L. Li.(2001). A comparative study of land surface emissivity retrieval from NOAA data. Remote Sensing of Environment, 75, pp. 256–266.

Su, Z. (2002). The Surface Energy Balance System (SEBS) for estimation of turbulent heat fluxes. Hydrology and Earth System Sciences, 6, pp. 85–100.

Susskind, J., Rosenfield, J., Reuter, D., and Chahine, M. T.(1984). Remote sensing of weather and climate parameters from HIRS2/MSU on TIROS-N. Journal of Geophysical Research, 89, pp. 4677–4697.

Tonooka, H. (2001). An atmospheric correction algorithm for thermal infrared multispectral data over land - A water-vapor scaling method. IEEE Transactions on Geoscience and Remote Sensing, 39, pp. 682–692.

Ulivieri, C., Castronuovo, M. M., Francioni, R., and Cardillo, A.(1996). A split-window algorithm for estimating land surface temperatures from satellites. Advan. Space Res., 14, pp. 1279-1292.

Valor, E. and V. Caselles.(1996). Mapping land surface emissivity from NDVI: Application to European, African and South American areas. Remote Sensing of Environment, 57, pp. 167−184.

Vauclin, M., Vieira, R., Bernard, R., and Hatfield, J. L. (1982). Spatial variability of surface temperature along two transects of a bare. Water Resources Research, 18, pp. 1677–1686.

Vidal, A.(1991). Atmospheric and emissivity correction of land surface temperature measured from satellite using ground measurements or satellite data. International Journal of Remote Sensing, 12, pp. 2449–2460.

Voogt, J. A., and Oke, T. R.(2003). Thermal remote sensing of urban climates. Remote Sensing of Environment, 86, pp. 370–384.

Wan, Z., and Dozier, J.(1996). A generalized split-window algorithm for retrieving land-surface temperature from space. IEEE Transactions on Geoscience and Remote Sensing, 34, pp. 892–905.

Wan, Z., and Li, Z.-L.(1997). A physics-based algorithm for retrieving land-surface emissivity and temperature from EOS/MODIS data. IEEE Transactions on Geoscience and Remote Sensing, 35, pp. 980–996.

Weng, Q.(2009). Thermal infrared remote sensing for urban climate and environmental studies: methods, applications, and trends. ISPRS Journal of Photogrammetry and Remote Sensing, 64, pp. 335–344.

Weng, Q.(2009). Thermal infrared remote sensing for urban climate and environmental studies: Methods, applications and trend ISPRS Journal of Photogrammetry and Remote Sensing, 64, pp. 335-344.

Weng, Q., Lu, D., and Schubring, J.(2004). Estimation of land surface temperature vegetation abundance relationship for urban heat island studies. Remote Sensing of Environment, 89, pp. 467–483.

Zhang Zhao-ming, H.E. Guo-jin, Xiao Rong-bo, Wang Wei and Ouyang ZhiYun. (2006). Land Surface Temperature Retrieval of Beijing city using MODIS and TM Data. Geoscience and Remote Sensing Symposium, IGARSS. IEEE International Conference on, pp. 1094-1096, 2006.

Zhang, R., Tian, J., Su, H., Sun, X., Chen, S., and Xia, J.(2008). Two improvements of an operational two-layer model for terrestrial surface heat flux retrieval. Sensors, 8, pp. 6165–6187.